Dynamical Mountain Meteorology

Dr. Yuh-Lang Lin, ylin@cat.edu; http://mesolab.org
Department of Physics/Department of Energy & Environmental Systems
North Carolina A&T State University
(Ref.: *Mesoscale Dynamics*, Y.-L. Lin, Cambridge, 2007)

Chapter 8 Two-Dimensional Flow over Isolated Mountains

5.2 Two-Dimensional Flow over Isolated Mountains

(5.2 Flows over two-dimensional isolated mountains – Lin 2007)
(Classical equation editor: $c_p \neq f(k)$)

5.2.1 Uniform basic flow

The mountain wave problem in Section 5.1 may be extended to be more realistic by assuming an isolated mountain.

Taking the one-sided Fourier transform (Appendix 5.1) of (5.1.5)

$$\nabla^2 w' + l^2(z) w' = 0\,, \qquad (5.1.5)$$

where $\nabla^2 = \partial^2/\partial x^2 + \partial^2/\partial z^2$ and

$$l^2(z) = \frac{N^2}{U^2} - \frac{U_{zz}}{U}\,. \qquad (5.1.6)$$

[Note that $l^2 = N^2/U^2$ is constant for a uniform flow, as assumed in Sec. 5.2.1]

Appendix 5.1: Some mathematical techniques and relations

(a) Fourier Transform

The Fourier transform of $f(x)$ is defined as

$$\hat{f}(k) = \frac{1}{2\pi}\int_{-\infty}^{\infty} f(x)\, e^{-ikx} dx \quad \text{and} \qquad \text{(A5.1.1a)}$$

$$f(x) = \int_{-\infty}^{\infty} \hat{f}(k)\, e^{ikx} dk\,. \qquad \text{(A5.1.1b)}$$

One of the advantages of the Fourier transform is that it can distinguish the upward- and downward propagation of wave energy.

An alternative Fourier transform pair may be defined as

$$\hat{f}(k) = \frac{1}{2\pi}\int_{-\infty}^{\infty} f(x)\, e^{-ikx} dx \quad \text{and} \qquad \text{(A5.1.2a)}$$

$$f(x) = 2\,\mathrm{Re}\int_{0}^{\infty} \hat{f}(k)\, e^{ikx} dk\,, \qquad \text{(A5.1.2b)}$$

for real function *f*. This is also called the one-sided Fourier transform (Queney et al. 1960).

Occasionally, the following pair of Fourier transform has been adopted in the literature,

$$\hat{f}(k) = \frac{1}{\pi}\int_{-\infty}^{\infty} f(x)\, e^{-ikx} dx \quad \text{and} \qquad \text{(A5.1.3a)}$$

$$f(x) = \mathrm{Re}\int_{0}^{\infty} \hat{f}(k)\, e^{ikx} dk\,. \qquad \text{(A5.1.3b)}$$

Other variations of Fourier transform pairs, such as using e^{ikx} (e^{-ikx}) in the forward (inverse or backward) Fourier transform, have also been used in the literature. No matter which form of the Fourier transform is used, the Fourier transform pair should be able to transform the original function back to itself after performing the forward and inverse transforms.

Fourier transform is useful in helping solve differential equations. For example, see http://www.physics.ucf.edu/~schellin/teaching/phz3113/lec9-3.pdf

It yields

$$\hat{w}_{zz} + (l^2 - k^2)\hat{w} = 0\,. \qquad (5.2.1)$$

The Fourier transform of the linear lower boundary condition (homework), (5.1.10), is

$$\hat{w}(k, z=0) = ikU\,\hat{h}(k)\,. \qquad (5.2.2)$$

For constant Scorer parameter, the solution of (5.2.1) can be written into two parts,

$$\hat{w}(k,z) = \hat{w}(k,0)\,e^{i\sqrt{l^2-k^2}\,z} \quad \text{for} \quad l^2 > k^2 \ \text{and} \qquad (5.2.3a)$$

$$\hat{w}(k,z) = \hat{w}(k,0)\,e^{-\sqrt{k^2-l^2}\,z} \quad \text{for} \quad l^2 < k^2\,. \qquad (5.2.3b)$$

Taking the inverse one-sided Fourier transform (Appendix 5.1)

A reminder: The *one-sided Fourier transform* pair is defined as

$$\hat{f}(k) = \frac{1}{2\pi}\int_{-\infty}^{\infty} f(x)\,e^{-ikx}dx \qquad (A5.1.2a)$$

$$f(x) = 2\,\mathrm{Re}\int_0^{\infty} \hat{f}(k)\,e^{ikx}dk \qquad (A5.1.2b)$$

of (5.2.3) yields the solution in the physical space,

$$w'(x,z) = 2\,\mathrm{Re}\left[\int_0^l ikU\;\hat{h}(k)\;e^{i\sqrt{l^2-k^2}\,z}e^{ikx}dk + \int_l^{\infty} ikU\;\hat{h}(k)\;e^{-\sqrt{k^2-l^2}\,z}e^{ikx}dk\right], \qquad (5.2.4)$$

where Re represents the real part.

The first integration on the right hand side of (5.2.4) represents the upward propagating wave which satisfies the upper radiation boundary condition, while the second integration represents the

evanescent wave which satisfies the boundedness upper boundary condition.

Note that (5.2.4) is for a continuous spectrum of Fourier modes, instead of just one single mode as considered in Sec. 5.1.

For simplicity, let us consider a bell-shaped mountain or the *Witch of Agnesi* mountain profile,

$$h(x) = \frac{h_m a^2}{x^2 + a^2}, \tag{5.2.5}$$

where h_m is the mountain height and a is the half-width where the mountain height is $h_m/2$.

The advantage of using a bell-shaped mountain lies in that its one-sided Fourier transform (Appendix 5.1)

> Again, the one-sided Fourier transform pair is defined as
>
> $$\hat{f}(k) = \frac{1}{2\pi}\int_{-\infty}^{\infty} f(x)\, e^{-ikx} dx \text{ and}$$
>
> $$f(x) = 2\,\mathrm{Re}\int_0^{\infty} \hat{f}(k)\, e^{ikx} dk,$$

is in a simple form,

$$\hat{h}(k) = \frac{h_m a}{2} e^{-ka}, \quad \text{for } k > 0. \tag{5.2.6}$$

The Fourier transform for any k is $(h_m a/2)\exp(-|k|a)$. (10/7/14)

Case 1: $l^2 << k^2$ (i.e., $al << 1$ or $Na << U$)

Note that for bell-shaped mountains, we assume $k \approx 1/a$, instead of $k = 2\pi/a$ for sinusoidal mountains.

As discussed earlier, the flow becomes a potential flow in which the buoyancy plays a negligible role. In this case, (5.2.4)

$$w'(x,z) = 2\,\mathrm{Re}\left[\int_0^l ikU\ \hat{h}(k)\ e^{i\sqrt{l^2-k^2}z} e^{ikx} dk + \int_l^\infty ikU\ \hat{h}(k)\ e^{-\sqrt{k^2-l^2}z} e^{ikx} dk\right], \quad (5.2.4)$$

can be approximated by

$$w'(x,z) \approx 2\,\mathrm{Re}\left[U\int_0^\infty ik\,\hat{h}(k)\,e^{-kz}e^{ikx}dk\right] = 2\,\mathrm{Re}\left[U\int_0^\infty ik\left(\frac{h_m a}{2}\right)e^{-ka}\,e^{-kz}e^{ikx}dk\right]. \quad (5.2.7)$$

Since $w' = U\partial\eta/\partial x$, the Fourier transform of η can be obtained from that of $\hat{w}$,

$$\hat{\eta}(k,z) = \frac{\hat{w}(k,z)}{ikU}. \quad (5.2.8)$$

Substituting (5.2.7) into (5.2.8) leads to

$$\eta(x,z) = h_m a\,\mathrm{Re}\int_0^\infty e^{-k(z+a-ix)}dk = \frac{h_m a(z+a)}{x^2+(z+a)^2}. \quad (5.2.9)$$

Therefore, similar to the sinusoidal mountain case, the flow pattern is symmetric with respect to the center of the mountain ridge ($x=0$). However, the amplitude decreases with height linearly, instead of exponentially. The flow pattern is depicted in Fig. 5.3a.

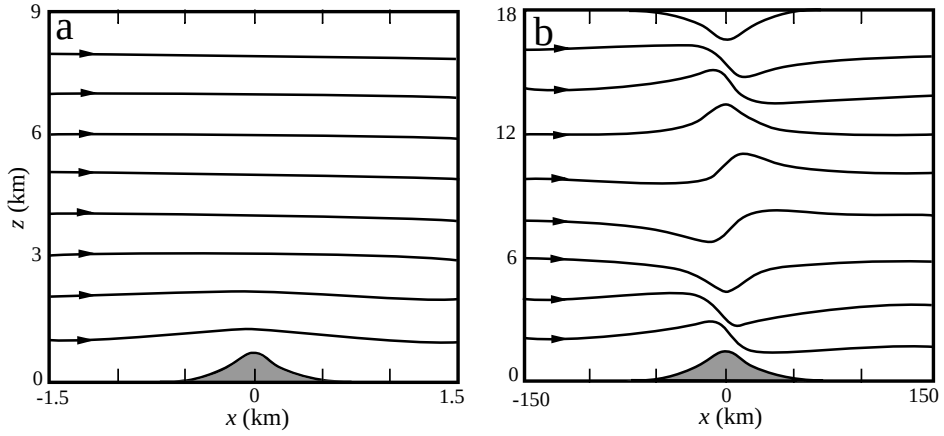

Fig. 5.3: Streamlines of steady state flow over an isolated, bell-shaped mountain when (a) $l^2 << k^2$ (or $Na << U$), where a is the half-width of the mountain, or (b) $l^2 >> k^2$ (or $Na >> U$). (Lin 2007; Adapted after Durran 1990)

Case 2: $l^2 >> k^2$ (i.e., $al >> 1$ or $Na >> U$)

As discussed in the previous section, the vertical acceleration due to the buoyancy force plays a dominant role.

In this case, the solution (5.2.4)

$$w'(x,z) = 2\,\mathrm{Re}\left[\int_0^l ikU\,\hat{h}(k)\,e^{i\sqrt{l^2-k^2}z}e^{ikx}dk + \int_l^\infty ikU\,\hat{h}(k)\,e^{-\sqrt{k^2-l^2}z}e^{ikx}dk\right], \qquad (5.2.4)$$

can be approximated by

$$w'(x,z) \approx 2\,\mathrm{Re}\left[U\int_0^\infty ik\hat{h}(k)e^{ilz}e^{ikx}dk\right] = 2\,\mathrm{Re}\left[U\int_0^\infty ik\left(\frac{h_m a}{2}\right)e^{-ka}e^{ilz}e^{ikx}dk\right]. \tag{5.2.10}$$

Similarly, the vertical displacement can be obtained,

$$\eta(x,z) = 2\,\mathrm{Re}\int_0^\infty \frac{h_m a}{2}e^{-ka}e^{i(kx+lz)}dk == \frac{h_m a(a\cos lz - x\sin lz)}{x^2+a^2}\,. \tag{5.2.11}$$

This type of flow is characterized as a hydrostatic mountain wave.

The disturbance confines itself over the mountain in horizontal, but repeats itself in vertical with a wavelength of $2\pi U/N$.

Without the Boussinesq approximation, the above solution becomes

$$\eta(x,z) = \left(\frac{\rho_s}{\rho(z)}\right)^{1/2}\left[\frac{h_m a(a\cos lz - x\sin lz)}{x^2+a^2}\right], \tag{5.2.12}$$

where ρ_s is the air density near surface.

Equation (5.2.12) indicates that the wave amplitude will increase with a decreased air density of the basic flow. That is, the wave amplitude will increase at higher altitudes since air density decreases with height in a stably stratified flow.

This helps explain the wave amplification in the higher atmosphere, such as large-amplitude gravity waves in the stratosphere, which causes aviation turbulence leading to aviation hazards.

As described in the previous section, other fields can be obtained by the governing equations, (5.1.1)-(5.1.4) with $U_z = 0$ (no basic wind shear).

The wave drag on the mountain surface in this hydrostatic limit can be obtained by applying the *Parseval theorem* (Appendix 5.1),

$$D = \int_{-\infty}^{\infty} p'(x, z=0)\frac{dh}{dx}dx = \int_{-\infty}^{\infty} p'(x,0)\frac{dh^*}{dx}dx = \frac{\pi}{4}\rho_o U N h_m^2, \tag{5.2.13}$$

where h^* is the complex conjugate of h. The momentum is transferred to a level where the wave breaks down, which is not included in the linear theory.

Case 3: $l^2 \approx k^2$ (i.e., $al \approx 1$ or $Na \approx U$)

An asymptotic solution can be obtained for this case. In this case, all terms of the vertical momentum equation, (5.1.2) are equally important. Both asymptotic methods and numerical methods have been applied to solve the problem.

In the following, we apply the *stationary phase method* to this particular problem. We look for solutions far downstream,

$x \to \infty$ in (5.2.4). In this limit, the second term on the right side of (5.2.4)

$$w'(x,z) = 2\,\mathrm{Re}\left[\int_0^l ikU\ \hat{h}(k)\ e^{i\sqrt{l^2-k^2}z} e^{ikx} dk + \int_l^\infty ikU\ \hat{h}(k)\ e^{-\sqrt{k^2-l^2}z} e^{ikx} dk\right],$$

approaches 0 due to fast oscillation of $\exp(ikx)$, according to the *Riemann-Lebesgue Lemma* (Appendix 5.1).

> ***(c) Riemann–Lebesgue Lemma***
>
> $$\lim_{x\to\infty} \int_{-\infty}^{\infty} \hat{f}(k) e^{ikx} dk = 0 \quad \text{if} \quad \hat{f}(k) \text{ is smooth.} \qquad \text{(A5.1.5)}$$
>
> A smooth function here means that the function is ordinary and absolutely integrable. The above conclusion is reached by the reasoning of cancellation.

Thus, for large x, we have

$$\eta(x,z) \approx 2\,\mathrm{Re} \int_0^l \hat{h}(k) e^{i\phi(k)} dk, \qquad (5.2.14)$$

where

$$\phi(k) = \sqrt{l^2 - k^2}\, z + kx \qquad (5.2.15)$$

is a *phase function*. Based on the stationary phase method, we will look for a particular k^* such that

$$\frac{d\phi}{dk} = 0 \quad \text{at} \quad k = k^*, \qquad (5.2.16)$$

where k^* is called the point of stationary phase.

With large *x* or *z*, $\exp(i\phi)$ will oscillate rapidly and, therefore, η will approach 0, according to Riemann-Lebesgue Lemma. However, near k^*, the contribution to the integration by $\exp(i\phi)$ still remains because ϕ is approximately constant.

Substituting the phase function (5.2.15) into (5.2.16) leads to the *influence function*,

$$\frac{z}{x} = \frac{\sqrt{l^2 - k^{*2}}}{k^*}, \tag{5.2.17}$$

in the region near k^*.

Taking the *Taylor's series expansion* of $\phi(k)$ near k^* gives

$$\phi(k) = \phi(k^*) + \left[\frac{\partial \phi}{\partial k}\right]_{k^*} \tilde{k} + \frac{1}{2!}\frac{\partial^2 \phi}{\partial k^2}\tilde{k}^2 + \ldots, \tag{5.2.18}$$

where $\tilde{k} = k - k^*$.

The second term on the right side of the above equation disappears due to the definition of k^* in (5.2.16). Thus, (5.2.14) becomes

$$\eta(x,z) = 2\,\mathrm{Re}\left[\hat{h}(k^*)e^{i\phi(k^*)}\int_0^l e^{i\phi_{kk}\tilde{k}^2/2}dk\right]. \tag{5.2.19}$$

For a bell-shaped mountain,

$$\eta(x,z) = \sqrt{2\pi}\; h_m a e^{-k^* a}\left[\frac{(l^2 - k^{*2})^{3/4}}{l z^{1/2}}\right]\cos\left(\sqrt{l^2 - k^{*2}}\, z + k^* x - \frac{\pi}{4}\right), \qquad (5.2.20)$$

where

$$k^* = \frac{l}{\sqrt{(z/x)^2 + 1}}. \qquad (5.2.21)$$

Figure 5.4 shows an example of a flow over a ridge of intermediate width ($l^2 \approx k^2$) where the buoyancy force is important, but not so dominant that the flow becomes hydrostatic. The nearly periodic waves located to the upper right of the mountain are the *dispersive tail* of nonhydrostatic waves with k less than, but not much less than l.

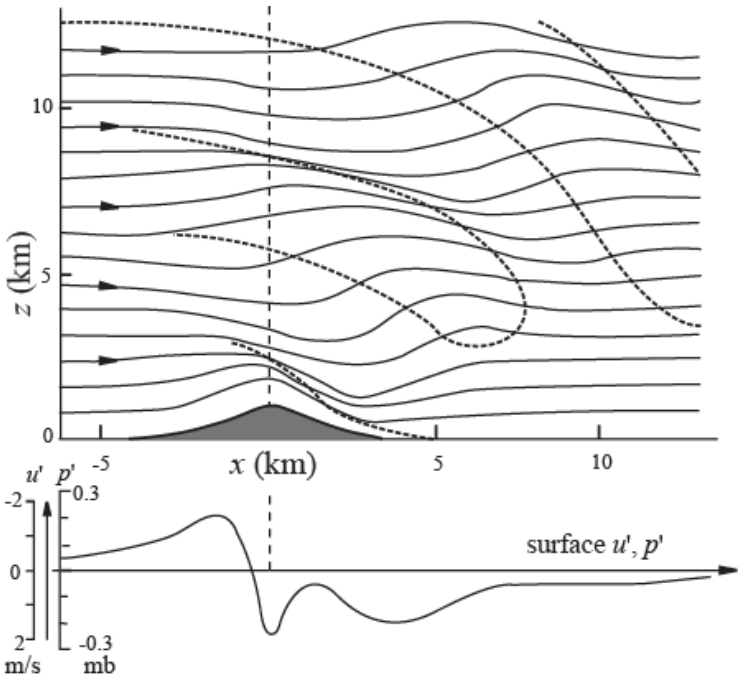

Fig. 5.4: Flow over a two-dimensional ridge of intermediate width ($l^2 \approx k^2$, or $al = Na/U = 1$) where the buoyancy force is important, but not so dominant that the flow is hydrostatic. The zero phase lines are denoted by dotted curves. The waves on the lee aloft are the *dispersive tail* of the nonhydrostatic waves ($k < l$, but not $k << l$). The flow and orographic parameters are: U = 10 ms^{-1}, N = 0.01 s^{-1}, h_m = 1 km, and a = 1 km. (Lin 2007; Adapted after Queney 1948)

In fact, the influence function, (5.2.17), is related to the energy propagation associated with the mountain waves. The group velocity (c_{gm}) in the frame of reference fixed with the mountain can be obtained from (3.5.11),

Eq. (3.5.11)

$$\Omega = \frac{\pm\ Nk}{\sqrt{k^2 + m^2}}$$

$$\boldsymbol{c}_{gm} = \left(U + \frac{\partial \omega}{\partial k} \right) \boldsymbol{i} + \frac{\partial \omega}{\partial m} \boldsymbol{k}, \tag{5.2.22}$$

where *m* in *gm* stands for mountain and

$$\omega = \frac{-Nk}{\sqrt{k^2 + m^2}}\,. \tag{5.2.23}$$

Substituting (5.2.23) into (5.2.22) leads to

$$\boldsymbol{c}_{gm} = U\boldsymbol{i} + \boldsymbol{c}_{ga} = \left[U - \frac{Nm^2}{(k^2 + m^2)^{3/2}} \right] \boldsymbol{i} + \left[\frac{Nkm}{(k^2 + m^2)^{3/2}} \right] \boldsymbol{k}, \tag{5.2.24}$$

where $\boldsymbol{c}_{ga}$ is the group velocity relative to the air.

Furthermore, the requirement of stationary waves, $c_{px} + U = 0$, implies

$$U = \frac{N}{\sqrt{k^2 + m^2}}. \qquad (5.2.25)$$

In (5.2.23), the negative sign is chosen in order to obtain positive c_{gz} by assuming positive k and m due to the use of one-sided Fourier transform.

The relationship among $c_{px}\boldsymbol{i}$, $\boldsymbol{c}_{gm}$ and $\boldsymbol{c}_{ga}$ is sketched in Fig. 5.5.

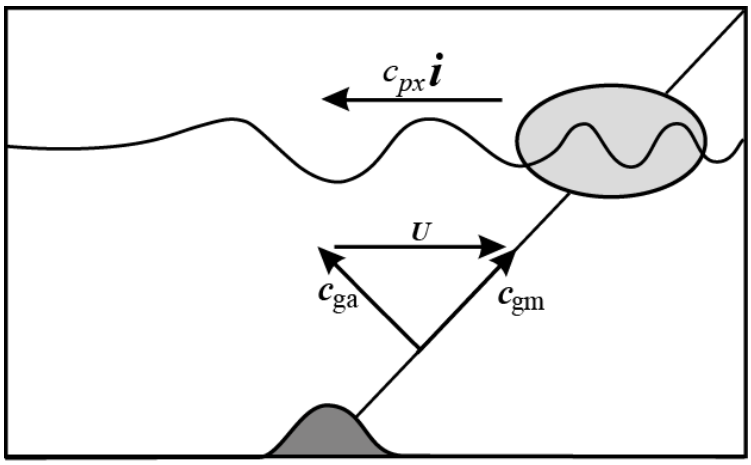

Fig. 5.5: A schematic illustrating the relationship among the group velocity with respect to (w.r.t) to the air ($\boldsymbol{c}_{\mathrm{ga}}$), group velocity w.r.t. to the mountain ($\boldsymbol{c}_{\mathrm{gm}}$), horizontal phase speed ($c_{px}\boldsymbol{i}$) and the basic wind. The horizontal phase speed of the wave is exactly equal and opposite to the basic wind speed. The wave energy propagates upward and upstream relative to the air, but is advected downstream by the basic wind. The energy associated with the mountain waves propagates upward and downstream relative to the mountain. (Lin 2007; After Smith 1979, reproduced with the permission from Elsvier.)

The upstream phase speed of the mountain wave is exactly equal to and opposite of the basic wind speed. The wave energy propagates upward and upstream relative to the air, but is advected downstream by the basic wind.

Thus, relative to the mountain, the energy associated with the mountain waves propagates upward and downstream. The slope of the group velocity can be obtained by substituting U of (5.2.25) into (5.2.24) and then calculating the slope,

$$\frac{c_{gz}}{c_{gx}} = \frac{m}{k} = \sqrt{\frac{N^2}{U^2 k^2} - 1} = \frac{\sqrt{l^2 - k^2}}{k} = \frac{z}{x}. \qquad (5.2.26)$$

In deriving the second equality, we have used (5.2.25), while in deriving the last equality, we have used (5.2.17) near the *point of stationary phase*, i.e. $k = k^*$.

Therefore, the point of stationary phase is the value of k corresponding to a wave with a group velocity beam as shown in Fig. 5.5. Waves are found downstream since the horizontal group velocity is less than the phase speed.

For general cases, such as $l^2 < k^2$ or $l^2 > k^2$, it is not easy to obtain analytical solutions from (5.2.4). With the advancement of numerical techniques, such as the Fast Fourier Transform (FFT) and computers, solutions can be approximately obtained numerically with the implementation of proper boundary conditions.

5.2.2 Basic flow with variable Scorer parameter

In the real atmosphere, the basic wind and stratification normally vary with height. To study the mountain waves produced by this type of basic flow, we assume that the Scorer parameter, (5.1.6), is a slowly-varying function of z .

In this situation, we expect to find a solution of (5.2.1)

$$\hat{w}_{zz} + (l^2 - k^2)\hat{w} = 0. \quad (5.2.1)$$

in form of,

$$\hat{w}(k,z) = \mathcal{A}(k,z)\, e^{i\phi(k,z)}, \quad (5.2.27)$$

where $\mathcal{A}(k,z)$ is a slowly varying amplitude function, and $\phi(k,z)$ is the slow-varying phase function. Substituting (5.2.27) into (5.2.1) yields

$$\left[-\mathcal{A}\phi_z^2 + (l^2 - k^2)\mathcal{A}\right] + i(\mathcal{A}\phi_{zz} + 2\mathcal{A}_z\phi_z) + \mathcal{A}_{zz} = 0. \quad (5.2.28)$$

The last term makes a minor contribution and can be neglected, since $A(k,z)$ is a slow-varying function of z. Thus, the above equation reduces to

$$\phi_z = \sqrt{l^2 - k^2}\,, \text{ and} \quad (5.2.29)$$

$$\frac{\partial}{\partial z}(\mathcal{A}^2\phi_z) = 0 . \qquad (5.2.30)$$

Combining the above two equations leads to

$$\mathcal{A}^2\sqrt{l^2 - k^2} = constant . \qquad (5.2.31)$$

For long (hydrostatic) waves ($l^2 >> k^2$), the above equation reduces to

$$\mathcal{A}^2 l = constant . \qquad (5.2.32)$$

This implies that the amplitude of the vertical velocity increases (decreases) significantly in regions of weak (strong) stratification or strong (weak) wind.

For example, the mountain wave tends to steepen when it propagates to the region below a jet stream or a jet streak since the basic wind speed increases there.

Note that in applying (5.2.27) to solve the problem, and in neglecting the last term of (5.2.28), we have implicitly adopted a first-order WKBJ approximation.

A second-order WKBJ approximation has been used to calculate wind profile effects on mountain wave drag (e.g., Teixeira and Miranda 2006). It is necessary to extend the WKBJ approximation to second order for these effects to be taken into account.

Based on (5.2.32) and previous discussions, waves may amplify in certain layers due to: (a) weaker stratification, (b) stronger wind, such as a jet stream or jet streak, (c) nonlinear steepening, and (d) abrupt decrease in the mean density, leading to an increase of $\sqrt{\rho_s / \rho(z)}$, in (5.2.12). 10/15/14

5.2.3 Trapped lee waves

One of the most prominent features of mountain waves is the long train of wave clouds over the lee of mountain ridges in the lower atmosphere, such as those shown in Fig. 5.6.

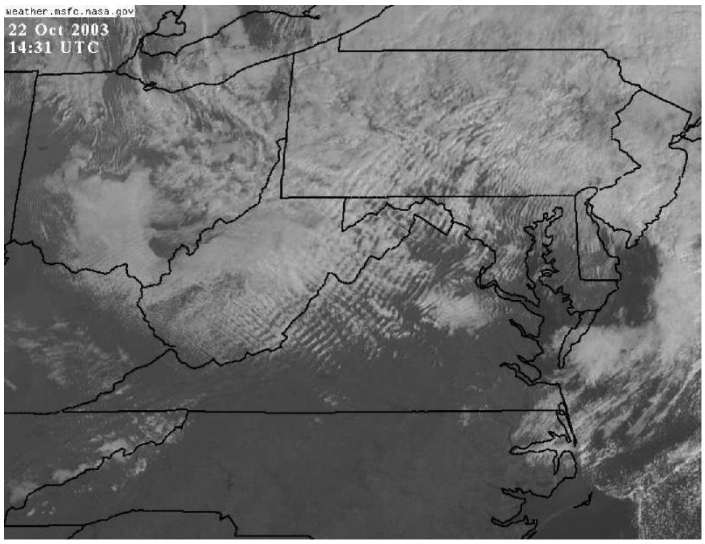

Fig. 5.6: Satellite imagery for lee wave clouds observed at 1431 UTC, 22 October 2003, over western Virginia. Clouds originate at the Appalachian Mountains. (Courtesy of NASA)

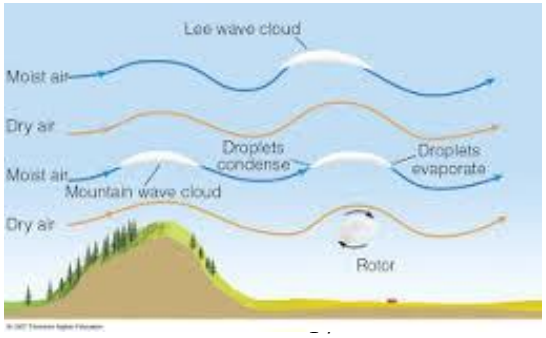

A schematic for lee waves and rotors

More pictures:
http://images.google.com/images?hl=en&q=lee+waves&um=1&ie=UTF-8&ei=dB-yS4f0OIWClAeF26HtBA&sa=X&oi=image_result_group&ct=title&resnum=4&ved=0CDYQsAQwAw

This type of wave differs from the dispersive tails in Fig. 5.4 in that it is located in the lower atmosphere and there is no vertical phase tilt.

It will be shown below that this type of trapped lee waves, or resonance waves, occurs when the Scorer parameter decreases rapidly with height (Scorer 1949).

The dynamics of trapped lee waves may be understood by considering a two-layer stratified fluid system. The wave equations for the vertical displacement in Fourier space may be written in a form similar to (5.2.1),

$$\hat{w}_{zz} + (l^2 - k^2)\hat{w} = 0. \quad (5.2.1)$$

$$\hat{\eta}_{zz} + [l_1^2 - k^2]\hat{\eta} = 0 \quad \text{for} \quad -H \le z < 0 \ \text{and} \qquad (5.2.33a)$$

$$\hat{\eta}_{zz} - [k^2 - l_2^2]\hat{\eta} = 0 \quad \text{for} \quad 0 \le z. \qquad (5.2.33b)$$

In this two-layer fluid system, we have assumed that $l_2^2 < k^2 < l_1^2$.

For convenience, the ground and the interface of the lower and upper layers are assumed to be located at $z = -H$ and $z = 0$, respectively.

The free wave solutions may be written as

$$\hat{\eta}_1(k,z) = C\left[\cos\mu z - \frac{\lambda}{\mu}\sin\mu z\right] \text{ and} \qquad (5.2.34a)$$

$$\hat{\eta}_2(k,z) = C\, e^{-\lambda z}, \qquad (5.2.34b)$$

where $\mu = \sqrt{l_1^2 - k^2}$, $\lambda = \sqrt{k^2 - l_2^2}$ and C is a constant coefficient to be determined by the lower boundary condition.

The boundedness upper boundary condition has been applied to exclude the $\exp(\lambda z)$ term, and the kinematic and dynamic boundary conditions at the interface, i.e. the continuities of $\hat{w}$ and $\hat{w}_z$ at $z = 0$, have also been applied.

In order to obtain a complete solution of the boundary value problem for a specific obstacle, we may apply the linear lower boundary condition,

$$\hat{\eta}_1(k,-H) = \hat{h}(k). \qquad (5.2.38)$$

Substituting the above equation into (5.2.34) and taking the inverse Fourier transform of $\hat{\eta}(k,z)$ leads to the forced wave solution in the lower layer,

$$\eta_1(x,z) = 2\,\mathrm{Re}\int_0^\infty \frac{\hat{h}(k)(\cos\mu z - (\lambda/\mu)\sin\mu z)e^{ikx}}{(\cos\mu H + (\lambda/\mu)\sin\mu H)}\,dk\,. \qquad (5.2.39)$$

The singularity in the denominator of the above equation corresponds to the resonance mode that will produce lee waves.

Equation (5.2.39) can be solved asymptotically or numerically with a given mountain-shape function (Scorer 1949; Smith 1979). Without enforcing a lower boundary condition, (5.2.34) represents free waves associated with this two-layer fluid system.

The resonance waves are obtained by seeking the zeros of (5.2.34a) with $z = -H$,

$$\cot\mu H = -\lambda/\mu\,. \qquad (5.2.35)$$

The resonance wave number (k_r^*) may be obtained by solving the above equation either numerically or graphically.

The criterion for the existence of one or more resonance waves may be obtained (Scorer 1949):

$$l_1^2 - l_2^2 \geq \frac{\pi^2}{4H^2}\,. \qquad (5.2.36)$$

A more general criterion for resonance waves of the *n*th mode is

$$\left[\frac{(2n+1)\pi}{2H}\right]^2 \geq (l_1^2 - l_2^2) \geq \left[\frac{(2n-1)\pi}{2H}\right]^2. \qquad (5.2.37)$$

The above criterion implies that *in order to have resonance (lee) waves, the Scorer parameter in the lower layer must be much greater than that in the upper layer*.

In other words, the lower layer must be more stable or with a much slower basic wind speed than the upper layer.

Figure 5.7 shows lee waves simulated by a nonlinear numerical model for two-layer airflow over a bell-shaped mountain. Due to the co-existence of the upward propagating waves and downward propagating waves, there exists no phase tilt in the lee waves.

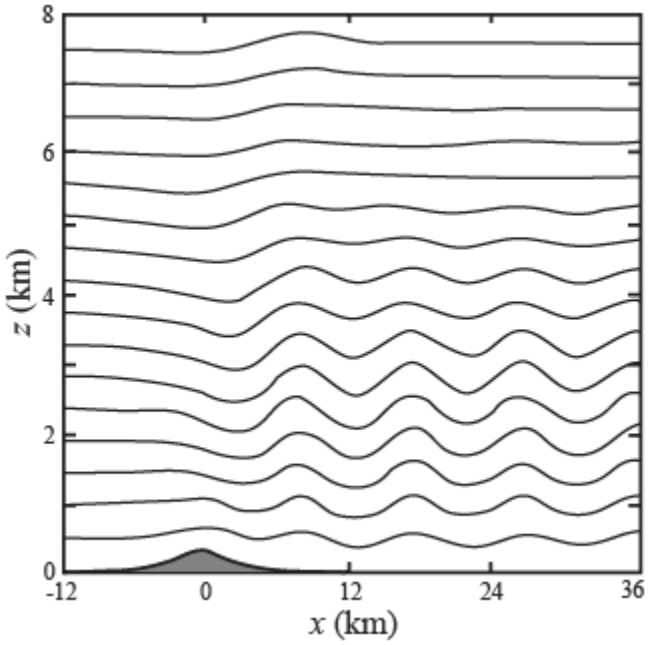

Fig. 5.7: Lee waves simulated by a nonlinear numerical model for a two-layer airflow over a bell-shaped mountain. Displayed are the quasi-steady state streamlines. In the lower layer (below 5 km approximately), $l^2 = 9x10^{-7}\,\mathrm{m}^{-2}$, while in the upper layer, $l^2 = 2x10^{-7}\,\mathrm{m}^{-2}$. (Lin 2007; Adapted after Durran 1986b)

Once lee waves form, regions of reversed cross-mountain winds near the surface beneath the crests of the lee waves may develop due to the presence of a reversed pressure gradient force.

In the presence of surface friction, a sheet of vorticity parallel to the mountain range forms along the lee slopes, which originates in the region of high shear within the boundary layer.

The vortex sheet separates from the surface, ascends into the crest of the first lee wave, and remains aloft as it is advected downstream by the undulating flow in the lee waves (Doyle and Durran 2004).

The vortex with recirculated air is known as *rotor* and the process that forms it is known as *boundary layer separation*, which will be further discussed in subsection 5.4.2 along with lee vortices.

These rotors are often observed to the lee of steep mountain ranges such as over the Owens Valley, California, on the eastern slope of Sierra Nevada (e.g., Grubišić and Lewis 2004). Occasionally, a turbulent, altocumulus cloud forms with the rotor and is referred to as *rotor cloud*.

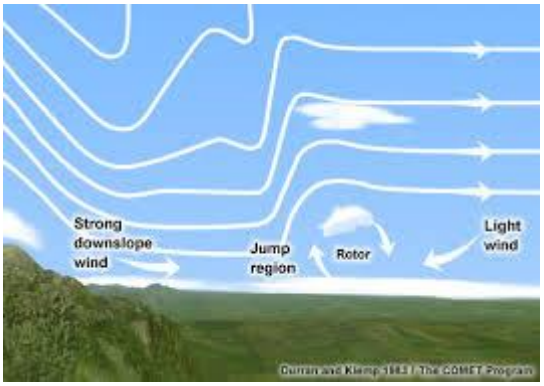

Some useful pictures of rotor clouds can be found at the following website:

- rotor clouds
- https://www.eol.ucar.edu/field_projects/t-rex (T-REX Field Experiment)
- http://opensky.library.ucar.edu/collections/OSGC-000-000-011-085 (T-REX mountain wave model intercomparison)